

SUPPLEMENTAL DATA

Cerebrovascular dysfunction and microcirculation rarefaction precede white matter lesions in a mouse model of CADASIL

Authors

Anne Joutel^{1,2,3}, Marie Monet-Leprêtre^{1,2*}, Claudia Gosele^{4*}, Céline Baron-Menguy^{1,2}, Annette Hammes⁴, Sabine Schmidt⁴, Barbara Lemaire-Carrette^{1,2}, Valérie Domenga^{1,2}, Andreas Schedl⁵, Pierre Lacombe^{1,2}, Norbert Hubner⁴

Supplementary Material and methods

In situ Hybridization

Paraffin sagittal brain sections (7 μ m) were dewaxed, rehydrated through an ethanol series, boiled in 10 mM citrate buffer, digested with proteinase K (20 μ g/ml), post-fixed in 4% paraformaldehyde and dehydrated. Sections were hybridized at 50°C overnight in buffer containing 2X SSC, 50% v/v de-ionised formamide, 10% w/v dextran sulfate, 1 mg/ml herring sperm DNA and 70 mM DTT. After hybridization, sections were stringently washed (30 min in 5X SSC at 50°C, 30 min in a buffer containing 2X SSC and 50% v/v formamide at 55°C and 15 min in 0.1X SSC at room temperature) and treated with 13 mg/ml Ribonuclease A. Dehydrated sections were exposed to Kodak Biomax Mr film for 2-4 days. After exposure, slides were dipped in liquid photographic emulsion (NTB2, Kodak) and exposed at 4°C for 18 days. Slides were developed using Kodak D-19, fixed using KODAK rapid fixer and counterstained with toluidine blue. Sections were examined with dark field and bright field illumination on a Leica DMR microscope.

Histology, immunohistochemistry and GOM deposits analysis

Histology. Mice were deeply anesthetized with sodium pentobarbital (80 mg/kg) and perfused transcardially with 50 ml of 0.1 M sodium phosphate buffer (PB) followed by 200 ml of 4% paraformaldehyde in PB. Tissues were postfixed for 24 h in 4% paraformaldehyde at 4°C and processed for paraffin embedding after sequential dehydration in ethanol. Brains samples were cut as serial sections (7 μ m) in the sagittal plane. Sections were stained with hematoxylin and eosin (H&E), Klüver-Barrera Luxol fast blue to visualize myelin or Masson's trichrome to visualize vessel wall fibrosis. Sections were examined on a Nikon eclipse 80i microscope. Sections were obtained from at least 3 mice per genotype at each age and at least 12 sections of each mouse were examined.

SM-MHC and GFAP immunostaining. Paraffin sections were rehydrated and endogenous peroxidase blocked by incubation with hydrogen peroxide 3% in PBS 1X. Sections were blocked with 10% fetal bovine serum in PBS 1X, then incubated with rabbit anti-SMMHC (1:100 dilution, Biomedical Technologies Inc.) or rabbit anti-GFAP (1:4000 dilution, Sigma) in reaction solution (10% fetal bovine serum in PBS 1X) overnight at 4°C, and incubated with biotinylated anti-rabbit antibody. Immunoreactivity was visualized with avidin/biotin-horseradish peroxidase complex (Vectastain ABC-HRP kit, Vector Laboratories) and

developed with 3,3'-diaminobenzidine (DAB, Sigma). Hematoxylin counterstaining was used to provide cytological detail. All primary antibody concentrations were titrated to provide optimal staining.

Notch3, Collagen IV, Perlecan, smooth muscle alpha-actin immunostaining. Mice were deeply anesthetized with sodium pentobarbital and perfused transcardially with 50 ml of PBS1X. Brain was half cut and stored at -80°C until ready for embedding in OCT medium. Acetone fixed cryosections were blocked by 5% bovine serum albumin (BSA) for 1 h at room temperature, incubated with the following primary antibodies (mouse monoclonal anti-Notch3^{ECD} (clone 5E1 (12), 1:10 dilution), rabbit polyclonal anti-Notch3^{TMIC} (Bc4 (12), 1:1000 dilution), rabbit polyclonal anti-collagen IV (1:50 dilution, Novotec), rat monoclonal anti-perlecan (clone A7L6, 1:1000 dilution, Chemicon), mouse monoclonal anti α -actin (clone 1A4, 1:200 dilution, Dako) in 0.2% BSA in PBS1X for 2 h at room temperature followed by a FITC or TRITC-conjugated appropriate secondary antibody (Jackson Immunoresearch laboratories, West Grove, PA) in 0.2% BSA for 2 h at room temperature. Nuclei were counterstained with DAPI. Sections were examined with a fluorescence microscope (Nikon eclipse 80i).

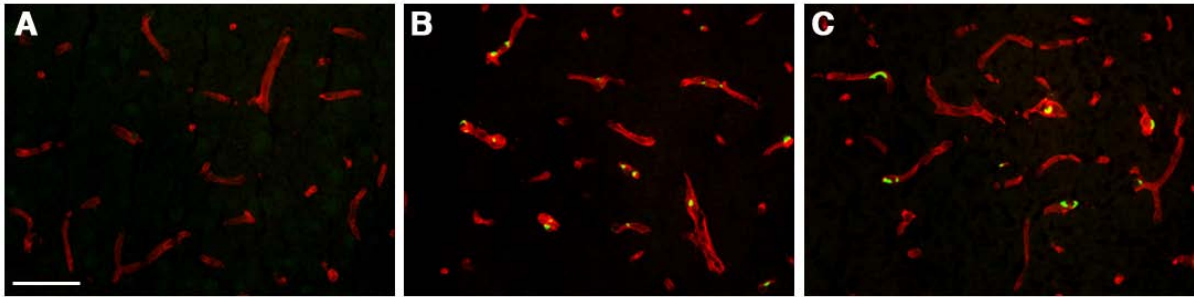
GOM deposits analysis. Trimmed sections (1-2mm thick) of tissues were fixed in a solution of CARSON as described and post-fixed in 2% osmium tetroxide in 0.1 M phosphate buffer pH 7.2. Samples were dehydrated with graded concentrations of alcohol and embedded in Epon. Semithin sections (1 μm) stained with toluidine blue were observed under a light microscope to select areas of interest. Ultrathin sections were cut and mounted on copper grids, contrasted with uranyl acetate and lead citrate and observed in a Philips CM100 electron microscope as described.

Analysis of cerebrovascular autoregulation and response to hypercapnia by laser Doppler flowmetry

Mice were held under minimal restraint and allowed to recover from anesthesia before tests during 2h after isoflurane was discontinued. Hypercapnia was induced by adding 5-7% CO_2 to the inhaled O_2/N_2 gas mixture for 2 min under the control of blood gases analysis. Mean arterial pressure was elevated by intravenous infusion of phenylephrine (40 $\mu\text{g}/\text{kg}$) up to 150 mmHg, and mean arterial pressure was decreased by controlled, stepwise exsanguination. Flow values from the two laser-Doppler flowmeter probes were averaged for each mouse. Changes in CoBF were expressed as percent change from baseline. The upper and lower limits of CoBF autoregulation were defined as the mean arterial blood pressure (MABP) at

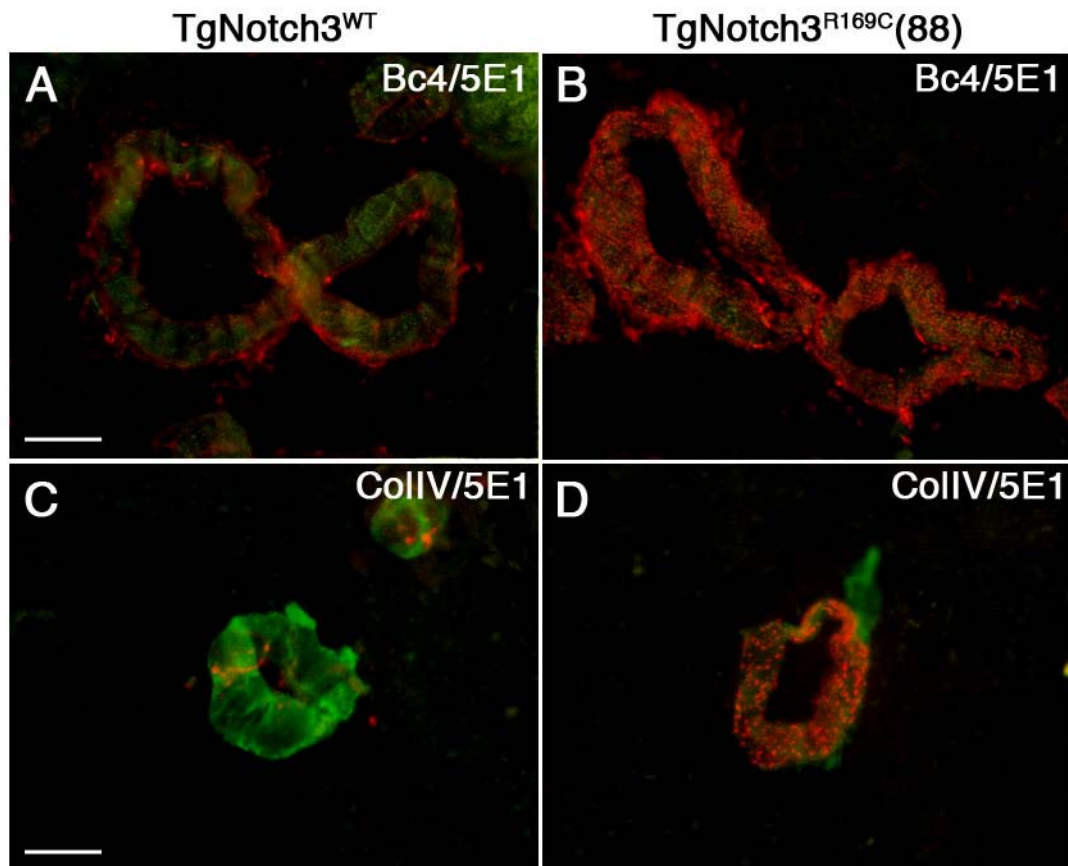
which CoBF goes above 110% or below 90% the baseline value, respectively. CO₂ reactivity was calculated by dividing the maximum plateau increase in CoBF percent change to the increase in arterial pCO₂ (mmHg) during hypercapnia.

Supplementary Figures



Supplementary figure 1: Notch3 expression in transgenic mice is confined to blood vessels. Double labeling for Notch3^{TMIC} (Bc4, green) and perlecan (red) in the brain of 1 month-old non-transgenic (A), TgNotch3^{WT} (B) and TgNotch3^{R169C} transgenic mice (C) showing that Notch3 expression in transgenic mice is confined to blood vessels. Endogenous Notch3 was not detected in this assay.

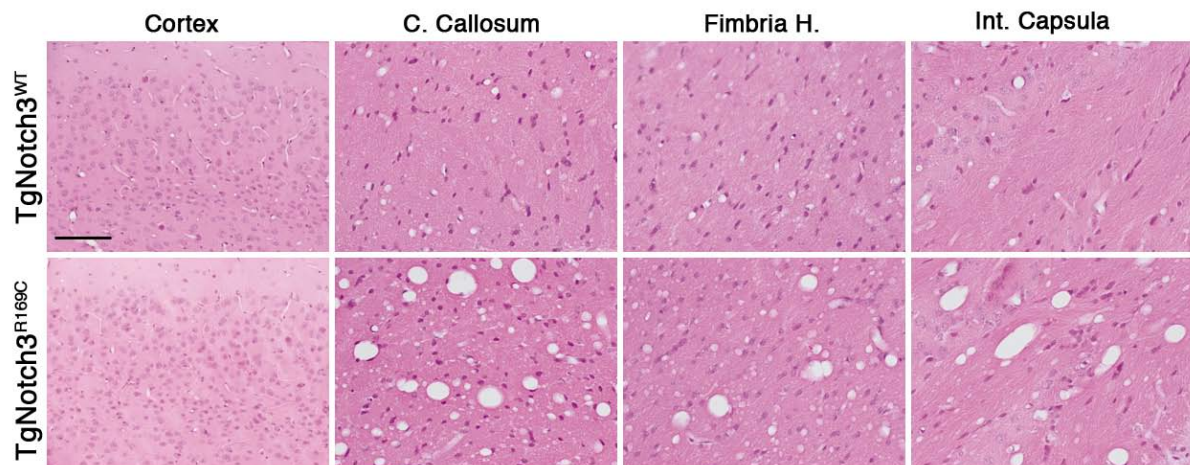
Scale bar is 55 μ m



Supplementary Figure 2: Robust accumulation of Notch3^{ECD} in arteries of aged TgNotch3^{R169C} mice

(A, B) Pial arteries of 20 month-old TgNotch3^{WT} (A) and TgNotch3^{R169C} (B) mice were double-stained with Notch3 antibodies specific to the intracellular (Bc4, green) or extracellular (5E1, red) domain. (C, D) Smaller brain arteries of 20 month-old TgNotch3^{WT} (C) and TgNotch3^{R169C} (D) mice were double stained with antibodies to Notch3 extracellular domain (5E1, red) and collagen IV (ColIV, green). Shown is robust aggregation of Notch3^{ECD} in the mutant arteries

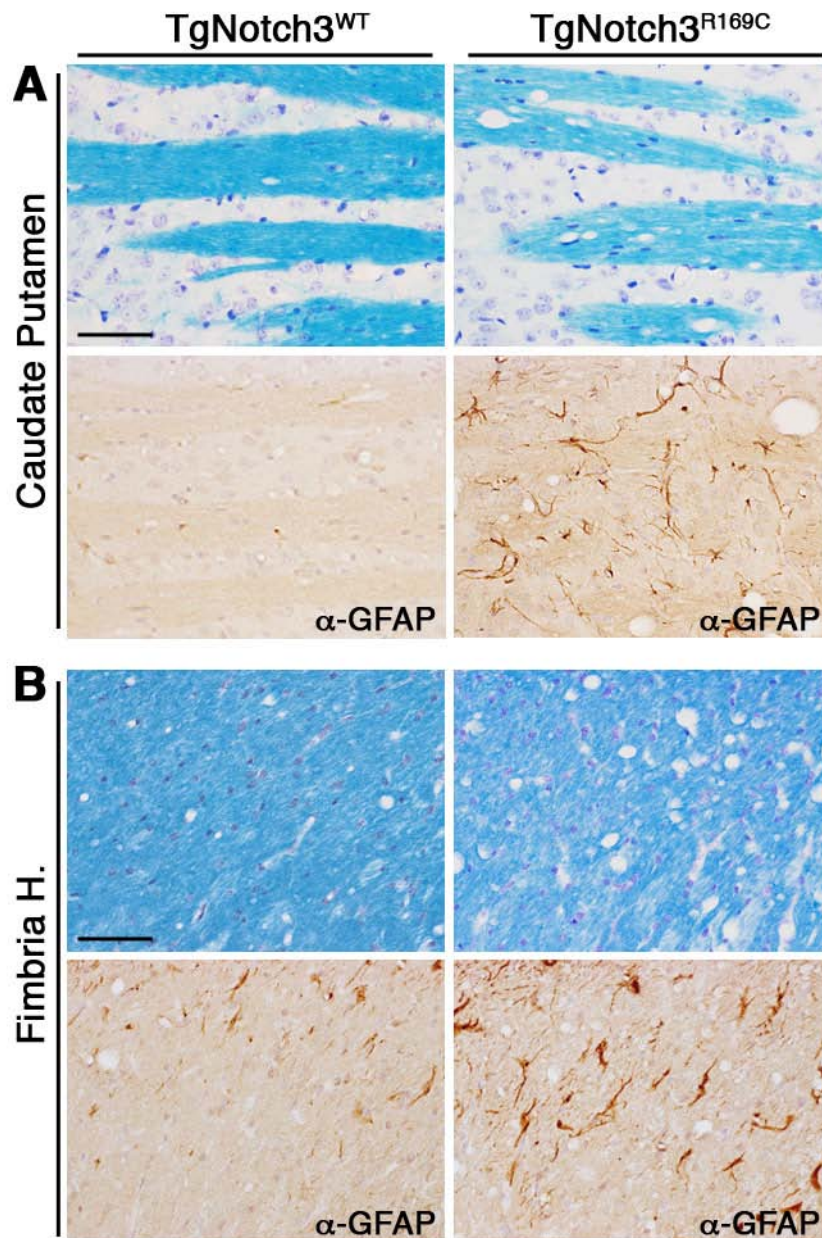
Scale bar is 25 μ m in (A, B) and 14 μ m in (C, D).



Supplementary Figure 3: Vacuolization of the white matter in 20 month-old TgNotch3^{R169C} mice

Shown are representative sections of the cortex, corpus callosum (C. Callosum), fimbria of the hippocampus (Fimbria H.) and internal capsula (Int. Capsula) from 20 month-old TgNotch3^{WT} and TgNotch3^{R169C} mice stained with Hematein & eosin.

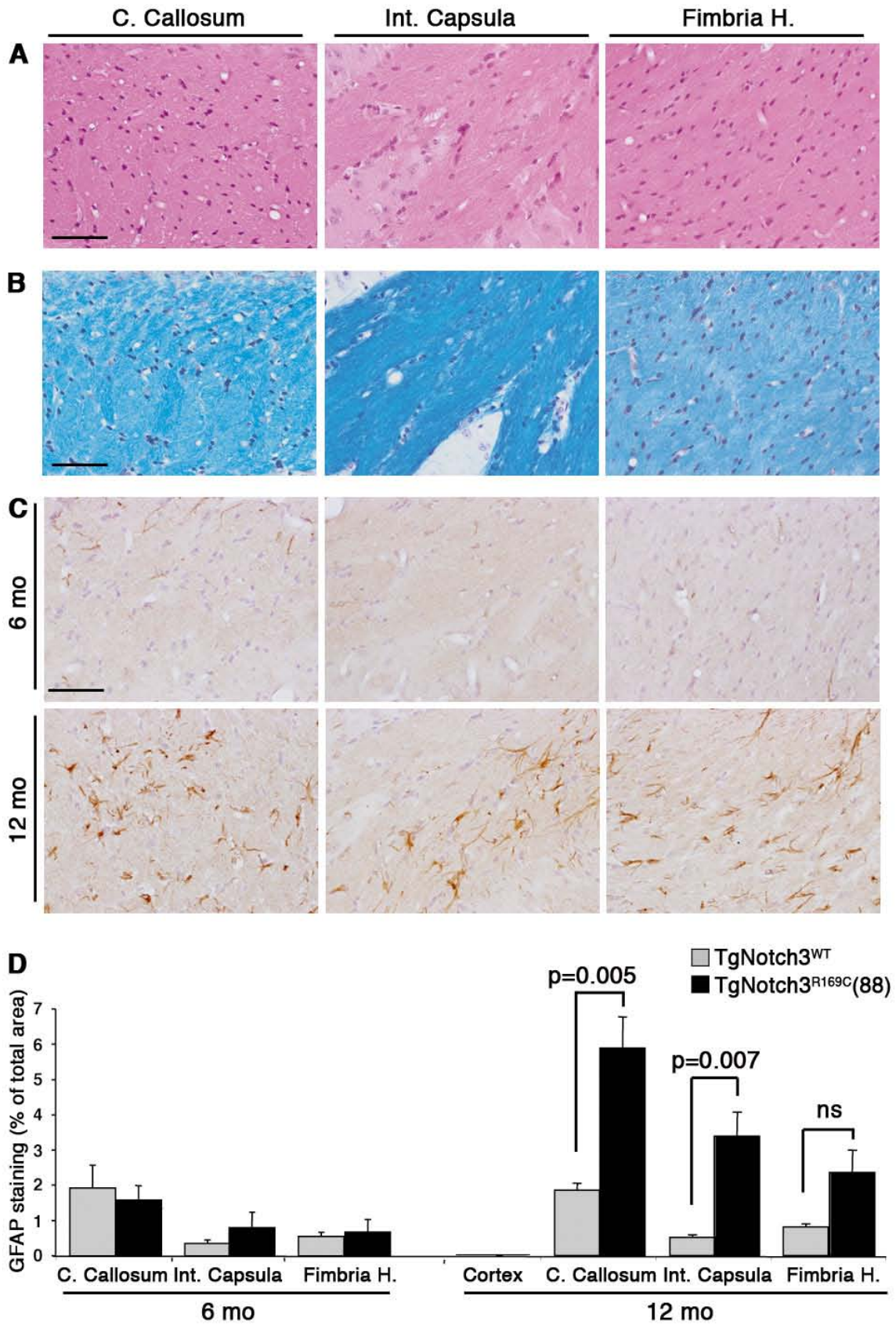
Scale bar is 65 μ m.



Supplementary Figure 4: White matter damages and astrogliosis in the caudate putamen and fimbria of hippocampus in 20 month-old TgNotch3^{R169C} mice

Shown are representative sections of caudate putamen (A) and fimbria of the hippocampus (B) from 20 month-old TgNotch3^{WT} and TgNotch3^{R169C} mice stained with Klüver-Barrera Luxol fast blue (upper panels) or GFAP (lower panels).

Scale bar is 65 μ m.



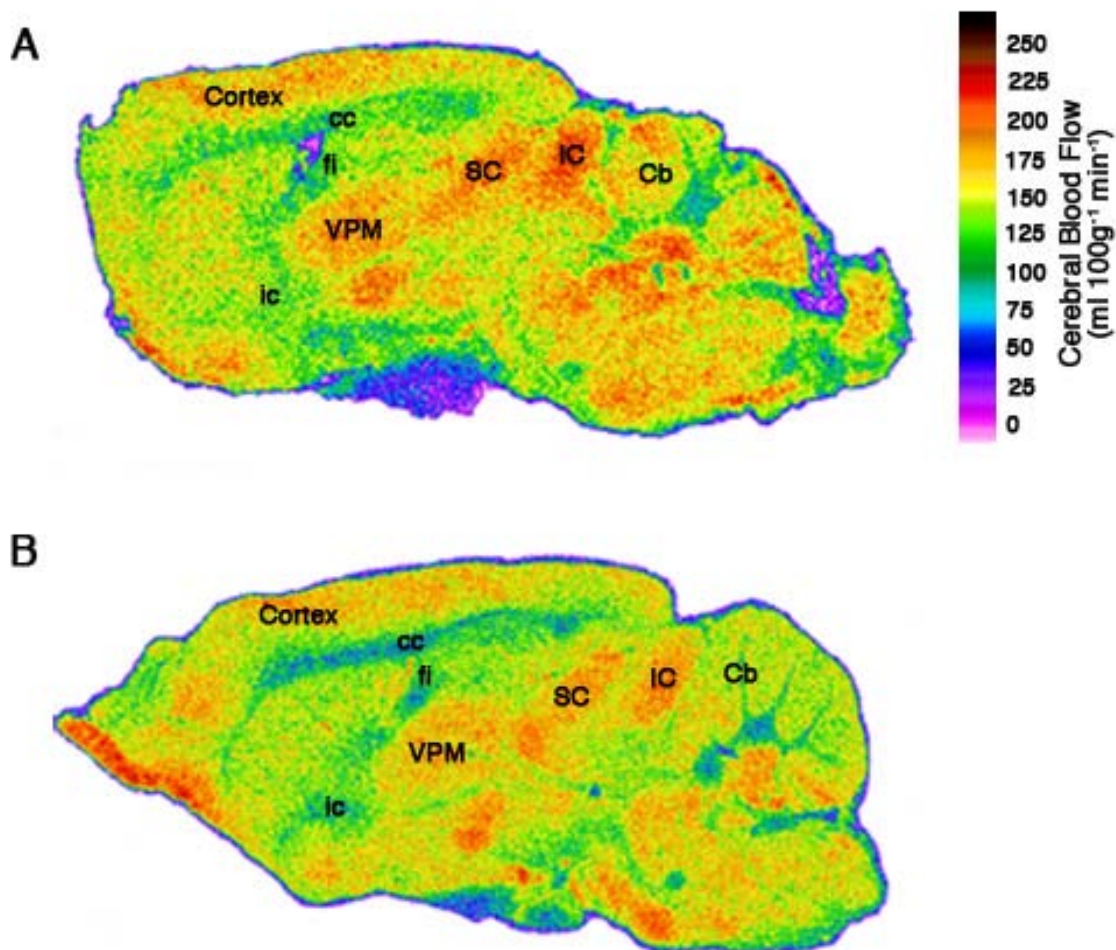
Supplementary Figure 5: Progressive astrogliosis in the white matter of TgNotch3^{R169C} mice prior to white matter disorganization and vacuolization

(A-B) Hematein & eosin staining (A) and Klüver-Barrera Luxol fast blue staining (B) in the corpus callosum, internal capsula and fimbria of the hippocampus of 12 month-old TgNotch3^{R169C} mice showing nearly intact parenchyma.

(C) GFAP staining in the corpus callosum, internal capsula and fimbria of the hippocampus of 6 (upper panels) and 12 month-old (lower panels) TgNotch3^{R169C} mice showing astrogliosis in mutant mice at 12 months of age, but not at 6 months of age.

(D) Quantification of astrogliosis in the cortex, corpus callosum, internal capsula and fimbria of the hippocampus of 6 and 12 month-old TgNotch3^{R169C} mice compared with TgNotch3^{WT} mice (n= 4-5 mice per group).

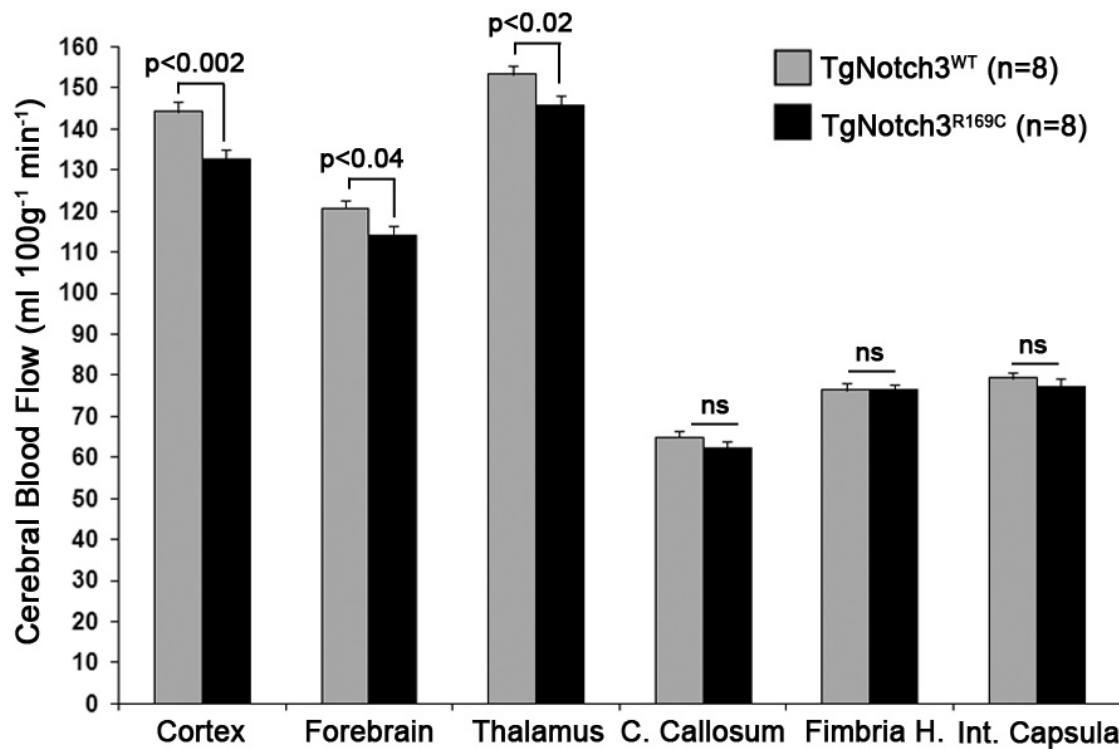
Scale bar is 65 μ m.



Supplementary Figure 6: Autoradiograms of regional cerebral blood flow

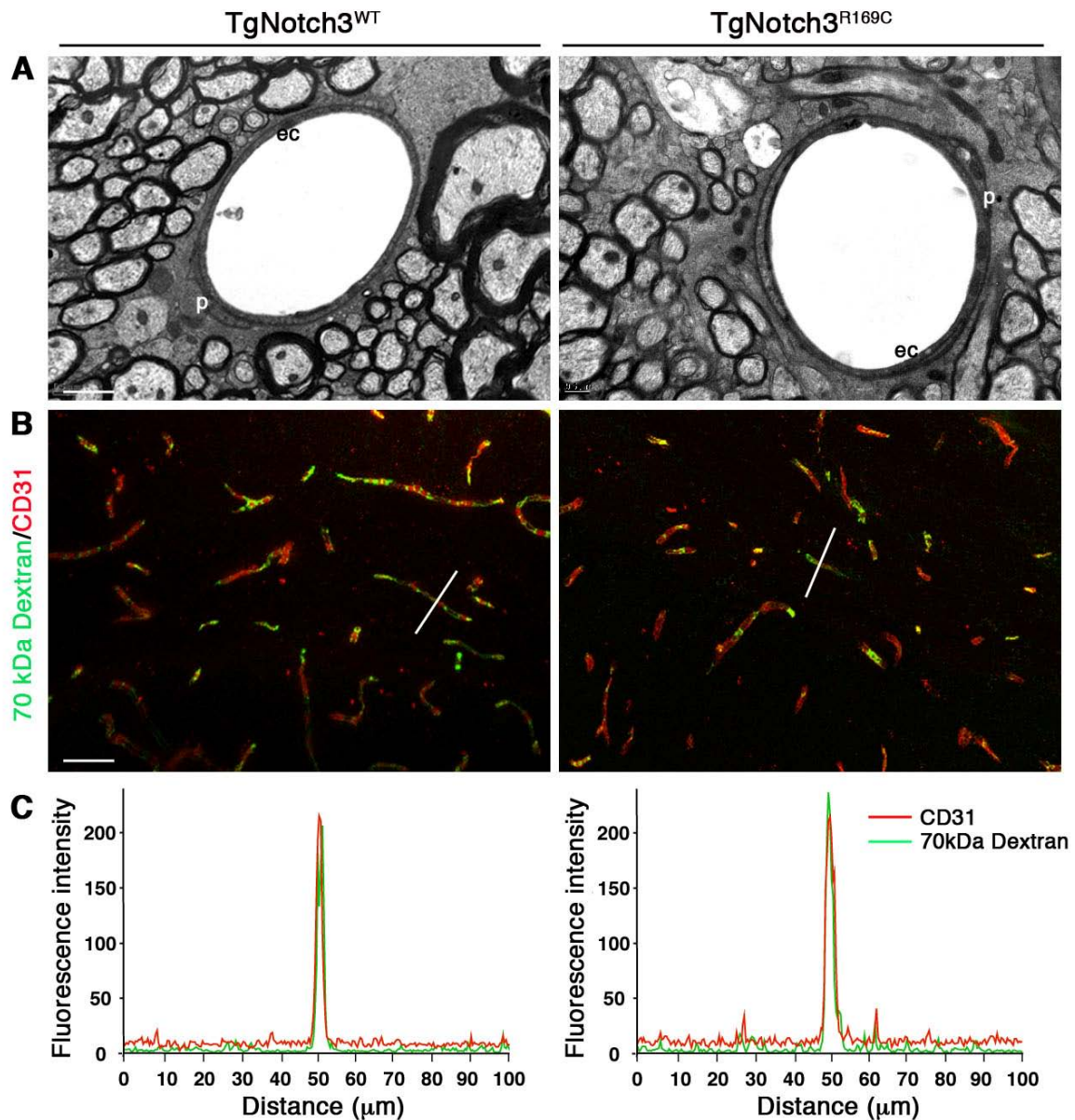
Representative blood flow autoradiograms (sagittal brain sections) in 18 month-old TgNotch3^{WT} (A) and TgNotch3^{R169C} (B) mice showing widespread reductions of blood flow in both gray and white matter regions in the mutant brain. The colored scale indicates absolute blood flow values.

Abbreviations: cb, cerebellum; cc, corpus callosum; fi, fimbria of the hippocampus; ic, internal capsule; IC, inferior colliculus ; SC, superior colliculus; VPM, ventral posteromedial thalamic nucleus.



Supplementary figure 7: Resting CBF in 11-12 month-old TgNotch3^{R169C} mice

Quantitative measurement of blood flow through the neocortex, forebrain (including the striatum, pallidum and amygdala), thalamus, corpus callosum (C. Callosum), fimbria of the hippocampus (Fimbria H.) and internal capsula (Int. Capsula) in 11-12 month-old TgNotch3^{R169C} compared with TgNotch3^{WT} mice shows comparable cerebral perfusion in the white matter of mutant and wild-type mice but hypoperfusion in the cortex, forebrain and thalamus of TgNotch3^{R169C} mice. Each of these large areas includes 8-10 gray matter regions or 4-5 white matter regions.

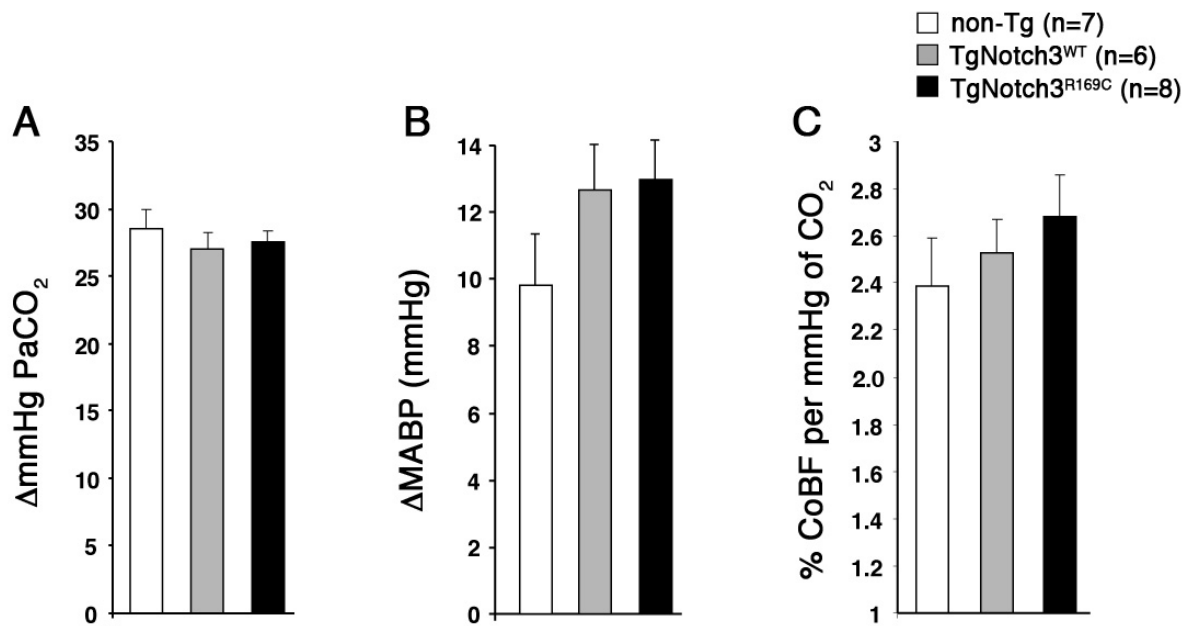


Supplementary Figure 8: Blood-brain barrier analysis of 12 month-old TgNotch3^{R169C} mice

(A) Representative electron micrographs of capillaries in the corpus callosum of 12 month-old TgNotch3^{R169C} and TgNotch3^{WT} (ec, endothelial cells; p, pericyte).

(B) Laser-scanning micrograph of microvasculature in the corpus callosum of 12 month-old TgNotch3^{R169C} and TgNotch3^{WT} mice injected with biotinylated-70kDa dextran 2 h before sacrifice. Sections were double labeled for CD31 (red) and biotinylated-dextran (green).

(C) Fluorescence intensity along a cross section (indicated by white bar) of a white matter capillary for the distribution of each fluorochrome showing no extravasation in the mutant vessel. Scale bar is 1 µm in (A) and 40 µm in (B).



Supplementary Figure 9: Cerebrovascular responses to Hypercapnia

Effects of hypercapnia (A) on arterial blood pressure (Δ MABP in mmHg, B) and CoBF (% change per mmHg of PaCO₂ increase, C) in 5 month-old TgNotch3^{R169C}, TgNotch3^{WT} and non-Tg mice. Responses were comparable in mutant and wild-type mice.

Supplementary Table 1: Physiological parameters in conscious, minimally restrained mice before quantitative regional cerebral blood flow measurements

	Non-Tg	TgNotch3 ^{WT}	TgNotch3 ^{R169C}	TgNotch3 ^{WT}	TgNotch3 ^{R169C}
Number of mice	7	8	7	9	8
Age (months)	18.3 ± 0.4	18.1 ± 0.4	17.7 ± 0.6	11 ± 0.2	10.9 ± 0.2
Hematocrit (%)	42.5 ± 1.0	40.7 ± 1.4	42.5 ± 1.0	45.7 ± 1.1	43.8 ± 0.3
pH	7.36 ± 0.009	7.34 ± 0.015	7.34 ± 0.013	7.30 ± 0.01	7.35 ± 0.01
PaO ₂ (mmHg)	86.7 ± 2.8	87.6 ± 2.8	94.6 ± 4.2	84.0 ± 1.7	90.0 ± 1.6
PaCO ₂ (mmHg)	36.8 ± 1.6	37.2 ± 0.6	37.0 ± 1.3	34.8 ± 0.8	34.3 ± 0.9
MABP (mmHg)	111.3 ± 2.1	112.7 ± 2.0	108.1 ± 2.5	108.7 ± 1.4	108.4 ± 1.8
Systolic BP (mmHg)	134.1 ± 2.3	134.9 ± 7.9	129.3 ± 3.4	128.5 ± 1.0	131.3 ± 2.3
Diastolic BP (mmHg)	91.1 ± 1.9	93.3 ± 2.0	93.3 ± 1.8	92.6 ± 1.7	93.3 ± 2.0
Heart rate (bpm)	694 ± 21	697 ± 23	709 ± 11	675 ± 18	643 ± 19

Values are means ± S.E.M . Group differences are not statistically different (one-way anova).

PaO₂ and PaCO₂, arterial pressure of O₂ and CO₂, respectively; MABP, mean arterial blood pressure

Supplementary Table 2: Physiological parameters in conscious, minimally restrained mice before determination of cerebral blood flow autoregulation and response to hypercapnia by laser-Doppler flowmetry

	Non-Tg	TgNotch3 ^{WT}	TgNotch3 ^{R169C}
Number of mice	7	6	7
Age (months)	5.0 ± 0.14	5.5 ± 0.09	5.3 ± 0.13
Body weight (g)	26.7 ± 1.36	27.2 ± 1.40	25.4 ± 0.44
Rectal temperature (°C)	37.8 ± 0.09	37.6 ± 0.11	37.8 ± 0.15
pH	7.34 ± 0.009	7.33 ± 0.02	7.33 ± 0.01
PaO ₂ (mmHg)	109.0 ± 4.7	114.3 ± 4.5	120.2 ± 2.4
PaCO ₂ (mmHg)	41.6 ± 1.47	43.9 ± 2.01	41.8 ± 1.14
MABP (mmHg)	100.6 ± 2.4	107.0 ± 4.1	103.3 ± 2.1
Systolic BP (mmHg)	117.7 ± 2.5	126.0 ± 4.7	121.5 ± 2.1
Diastolic BP (mmHg)	86.3 ± 1.5	91.5 ± 3.7	89.1 ± 1.7
Heart rate (bpm)	644 ± 18	588 ± 19	626 ± 21

Values are means ± SEM. Group differences are not statistically different (one-way anova).